AIP | Journal of Applied Physics

Adding 0.2V to the open circuit voltage of organic solar cells by enhancing the built-in potential

Nir Tessler

Citation: Journal of Applied Physics **118**, 215501 (2015); doi: 10.1063/1.4936367
View online: http://dx.doi.org/10.1063/1.4936367
View Table of Contents: http://scitation.aip.org/content/aip/journal/jap/118/21?ver=pdfcov
Published by the AIP Publishing

Adding 0.2 V to the open circuit voltage of organic solar cells by enhancing the built-in potential

Nir Tessler[a)]
Department of Electrical Engineering, Sara and Moshe Zisapel Nano-Electronic Center, Technion-Israel Institute of Technology, Haifa 32000, Israel

(Received 14 September 2015; accepted 11 November 2015; published online 1 December 2015)

We present a systematic device model that reproduces the important features of bulk heterojunction organic solar cells. While examining the model outputs we find that one of the limiting factors in organic solar cells is the reduced built-in potential due to effective pinning of the electrodes relative to the energy gap at the bulk of the device. Having identified this as a problem we suggest a device structure that can enhance the open circuit voltage. Our detailed modeling shows that such a structure can enhance the open circuit voltage as well as the short circuit current leading to above 40% improvement in power conversion efficiency of state of the art organic solar cells. © *2015 AIP Publishing LLC*. [http://dx.doi.org/10.1063/1.4936367]

INTRODUCTION

A significant fraction of the solar cell device research employs structures that do not rely on P-N architecture, but rather employ non doped layers as the active region. In the field of organic solar cells it is known that the loss of open circuit voltage, relative to the absorption gap, is too high. This is mainly evident in the ultimate efficiency[1–3] being well above reported values[4,5] and/or in the fact that an empirical loss of ca. 0.5 eV (Refs. 6–9) needs to be introduced. This gap between actual and theoretical values is often attributed to the active materials.[10–17] We find that a significant loss of an open circuit is due to the pinning of the electrode energy with respect to the bulk of the device which in turn limits the built-in potential. We show that a gradual change of the energy levels close to the contact interface allows for a wider energy gap between the electrodes thus inducing a higher built-in potential. We devise a new device structure that is able to recover 0.2 V of open circuit voltage as well as improve the fill factor such that ~48% could be added to the efficiency of state of the art cells (i.e., 10% would become 15%).

As we are concerned with improving the open circuit voltage of bulk heterojunction (BHJ) solar cells we first show that such improvement does not violate any physics law by repeating parts of Shockley and Queisser's paper[18] in the context of semiconductor device models, and in a simple form. We start with the generation recombination equation and the Boltzmann statistics that relate the Fermi level to the charge density.

$$\begin{cases} \dfrac{dn_{e,h}}{dt} = I - \dfrac{n_{e,h}}{\tau} \\ n_{e,h} = N_{C,V}\exp\left(-\dfrac{E_{C,V} - E_{Fe,h}}{kT}\right). \end{cases} \quad (1)$$

Here I is the charge generation rate, produced through the absorption of sun light, $n_e(n_h)$ is the electron (hole) density, τ is the charge recombination lifetime, $N_C(N_V)$ is the electron (hole) density of states, and $E_{Fe}(E_{Fh})$ is the quasi Fermi level of electrons (holes).

The electrochemical potential, $\Delta\mu$, which translates to an open circuit voltage (V_{OC}) is then calculated as

$$\begin{aligned} qV_{OC} = \Delta\mu = E_{Fe} - E_{Fh} &= Eg - kT\ln\left(\frac{N_C N_V}{n_e n_h}\right) \\ &= Eg - 2kT\ln\left(\frac{\sqrt{N_C N_V}}{I\tau}\right) \\ &\equiv Eg - 2kT\ln\left(\frac{\sqrt{N_C N_V}}{I_0\tau_0}\right) - 2kT\ln(\eta). \end{aligned} \quad (2)$$

Here Eg is the absorption gap energy, I_0 and τ_0 are some reference values, and η is a measure of deviation from them as in $\tau = \tau_0/\eta$. In Shockley and Queisser's paper[18] they show that knowing the properties of the Sun and of the semiconductor absorbing the light, it is possible to derive I_0 and τ_0 that represent the maximum theoretical efficiency of the solar cell. For the current discussion it suffices to consider that there exists a reference set of values that defines the minimal loss and that the loss of energy is measured relative to the absorption gap.

Next, we examine the issue of open circuit voltage through the ideal diode characteristics (Eq. (3.16) in Shockley and Queisser's paper[18]) that with some minor modifications also fits practical organic solar cells[19,20]

$$\begin{aligned} J &= J_0[\exp(qV/kT) - 1] - J_{SC} \\ &= -J_0 + J_0\exp(qV/kT) - J_{SC}. \end{aligned} \quad (3)$$

Here J_0 is the reverse saturation (or leakage) current, J_{SC} is the short circuit photocurrent, and V is the voltage drop across the cell. In Figure 1(a) we plot the last two terms on the right side of Equation (3) and extract graphically the open circuit voltage. A conclusion one may derive from Figure 1(a) is that it is the combination of the leakage current, J_0, and the short circuit current, J_{SC}, that dictates the open circuit voltage, V_{OC}. Another way to view the formation of the open

a)E-mail: nir@ee.technion.ac.il

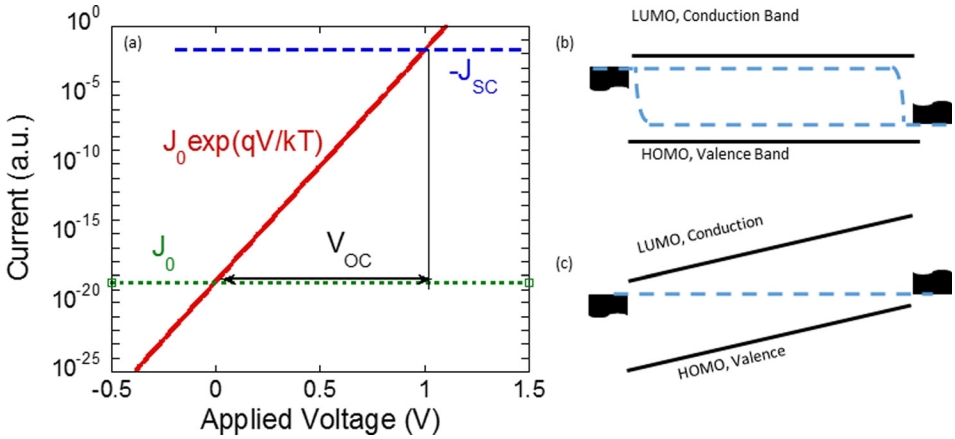

FIG. 1. (a) Schematic description of the last two terms on the right side of Equation (3). The leakage current (J_0) is in a dotted line, the exponentially rising diode current is in a solid line, and the short-circuit photocurrent (J_{SC}) is in a dashed line. (b) Schematic description of the energy band diagram at open circuit and sun illumination. (c) Schematic description of the energy band diagram at short circuit and in the dark. The dashed lines are the quasi Fermi levels.

circuit voltage is to compare the energy level diagram at short circuit and in the dark (Figure 1(c)) to the diagram at open circuit and under 1 Sun illumination (Figure 1(b)). For illustration we used here a metal-insulator-metal structure where the "insulator" is an undoped organic semiconductor and we assumed a low recombination in the bulk (i.e., high mobility). This is why at short-circuit the bands are not curved but tilted and at open circuit the bands are flat with the Fermi-level splitting in the bulk reflecting the open circuit voltage. The presence of dopants would create a Schottky type cell having a depletion layer[21] and a high recombination to mobility ratio would prevent the cell from reaching a flat band condition. See also Figure 5 in Ref. 22 that considered a p-i-n case.

At short circuit the equilibrium between the contacts dictates that the energy bands must be tilted, to level the two contacts. When the device is excited by the Sun it is filled with charges and at open circuit this charging rotates the bands to bring them to an almost flat (horizontal) condition. Comparing the two viewpoints we can conclude that just as J_0 affects the open circuit voltage so does the magnitude of the energy level tilt at short-circuit conditions. This last point would become important later in the text.

We claim that most of the discussion in the literature that has led large parts of the community to conclude that the reported V_{OC} is at its upper limit were mainly concerned with providing a solid physical ground for the J_{SC} part and by no means has anyone shown or claimed that the leakage currents obtained are at their minimum theoretical limit. In fact, Vandewal *et al.*[23] used the reciprocity relations[24] to represent the open circuit voltage as: $V_{OC} = V_{OC}^{rad} + kT\ln(EQE_{EL})$ and showed that the limiting factor is the low electroluminescence efficiency when operating as a light emitting diode (LED) (EQE_{EL}). In the context of that paper it is equivalent to stating that V_{OC} is limited by the leakage current. We remind the reader that in our discussion of Figure 1 we pointed out that the leakage current is related to the built-in potential. In other words, one can still enhance the open circuit voltage of BHJ cells by shifting the attention to the enhancement of the band bending at zero bias and consequently to the lowering of the leakage current. The above sentence is almost trivial and is well known but we will show a device structural design that would allow to go beyond what the standard structure can offer.

Below, we will argue that the pinning of the electrodes well within the gap[25,26] limits the open circuit voltage by forcing the built-in potential to be well below the electronic energy gap. Due to the nature of solar cells, a limit on V_{OC} has to be mirrored in enhanced recombination and in this case this is also so. We believe that part of the reason this mechanism has been overlooked is that the resulting extra-losses have the signature of bimolecular loss which one would expect to observe in a solar cell. We show the above by presenting results produced by a device model which incorporates the contacts in a self-consistent manner[27] and has recently been successfully used to analyze donor-acceptor bulk heterojunction devices.[28,29] As we will show below, this model includes the minimal number of physical processes that still allow it to capture the essence of the device performance.

RESULTS

To ensure that the model's results are on physical grounds we use the same assumptions as in Ref. 28 and similar parameters namely, we represent the bulk heterojunction as an effective medium consisting of a semiconductor with a suitable gap. To resemble the parameters used in Ref. 28 the effective band gap is taken to be 1.36 eV and the recombination is taken to be only the Shockley-Reed-Hall (SRH) type.[28,30,31] For the density at which the traps are full we use the value of $2n_i\cosh\left(\frac{\Delta E_t}{kT}\right) = 10^{15}\text{cm}^{-3}$ with ΔE_t being the trap position relative to the middle of the gap and n_i being the intrinsic charge density (i.e., due to the thermal excitation in the dark). The traps capture rate, which is the capture cross section (C_n) times the trap density (N_t), is taken initially to be relatively high as $C_nN_t = 3.3 \times 10^5\ \text{s}^{-1}$. We also assume one Sun illumination following an exponential type absorption, having an absorption depth of 150 nm and a total of 40% being converted into free carriers.

To check if the open circuit voltage may indeed be limited by the device structure we tested for the effect of varying two parameters. The first is the capture rate, C_nN_t (Figure 2(a)), dictating the recombination which is a material property and the second is the position of the contact work function (Figure 2(b)) relative to the band edge, which we consider to be a device property.

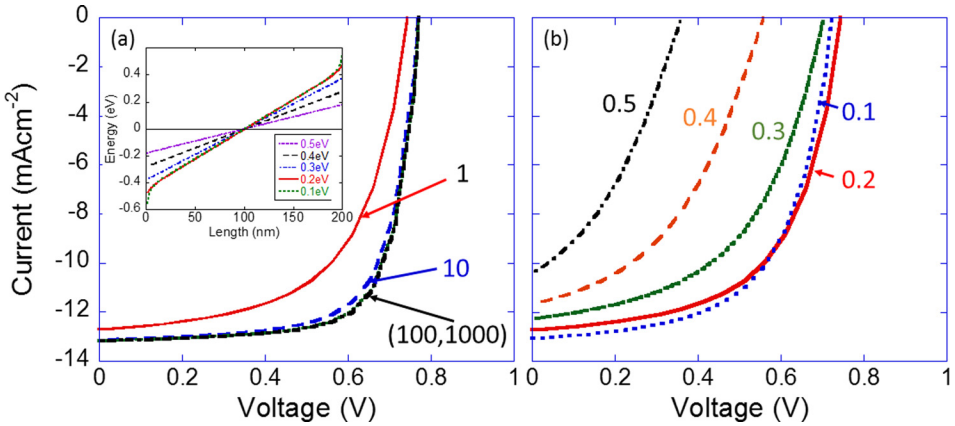

FIG. 2. (a) Simulated current voltage curves under one Sun illumination and for different SRH recombination rates. The solid line is for $C_nN_t = 3.3 \times 10^5\ s^{-1}$, the dashed line for a factor 10 reduction ($C_nN_t = 3.3 \times 10^4\ s^{-1}$), and the two overlapping lines are for 100 and 1000 fold reduction in C_nN_t. (b) Simulated current voltage curves under one Sun illumination and for different contact barrier heights at the two electodes. The solid line (0.2 eV) is identical to the solid one in (a) and the rest are for 0.5 eV, 0.4 eV, 0.3 eV, and 0.1 eV—as marked in the figure. The inset to (a) shows the band (LUMO) diagram at zero applied bias, under dark conditions, and for the set of barrier heights used in (b). For clarity, the reference potential is taken to be at the center of the device.

Figure 2(a) shows simulation results of the current voltage curves under one Sun illumination where the recombination rate was varied, starting from $C_nN_t = 3.3 \times 10^5\ s^{-1}$ and then reducing it by factors of 10, 100, and 1000. For this set the contacts were assumed to be positioned 0.2 eV within the gap making the electrode gap (E_{FMe}-E_{FMh}) $1.36 - 0.2 - 0.2 = 0.96$ eV (effective electronic band gap was taken to be 1.36 eV). The full set of parameters is tabulated in Table I in the Appendix. As indicated by Equation (2), if the performance was limited by the recombination lifetime then the open circuit voltage should have increased by steps of $2kT\ln(10) = 120$ meV. As the overall increase is only 30 meV it is clear that the factor limiting the open circuit voltage is not the trap assisted recombination lifetime. This result is similar to the experimental study by Cowan *et al.*[32] which showed that below $C_nN_t \sim 10^4\ s^{-1}$ the open circuit voltage is not affected by trap assisted recombination. In Cowan's paper however, the saturation of the open circuit voltage was attributed to bimolecular recombination in the bulk, which is not part of the model used here (we will discuss the mechanism at play in the device model later in the text).

In Figure 2(b) we show the simulation results of varying the contact barrier height from 0.5 eV to 0.1 eV while keeping the recombination rate constant at $C_nN_t = 3.3 \times 10^5\ s^{-1}$. We note that slightly below 0.3 eV the open circuit voltage practically saturates suggesting that the contacts or the pinning of the contacts within the gap is not a limiting factor either. However, as discussed in the review by Kahn *et al.*,[25] besides pinning at the interface there could be pinning with respect to the bulk of the device due to charge spillage into the semiconductor that forms a dipole like or space charge layer. This space charge bends the bands close to the contacts thus pushing the contact, relative to the bulk, into the gap creating a pinning effect (with respect to the energy level in the bulk of the device). This space charge induced pinning is the effect captured by our simulations and to demonstrate it we show in the inset of Figure 2(a) the band (LUMO) level at zero applied bias and under dark conditions. The various lines represent calculations for barrier heights of 0.5 eV–0.1 eV where, for illustration, the reference potential was chosen at the center of each device. Note that slightly below 0.3 eV the energy slope saturates indicating that the built in electric field at the bulk saturates or that the electrodes are being effectively pinned (by the space charge near the contacts). This means that the 0.96 eV we calculated above was the pinning-free energy gap between the contacts and that the actual gap is smaller, due to the space charge induced pinning. Summing up the results in Figure 2 we may conclude that at least part of the limit to the open circuit voltage is imposed by the contacts and as the internal losses are being reduced, the contacts become the dominant factor.

As discussed, in this minimal model, the losses in the bulk could arise only from SRH recombination. As we do not take the contacts to be blocking there would also be recombination at the contact interface. As this is a minimal model one needs to show that while being minimal it is sufficient to capture the essence of the solar cell being discussed. To do so we start by using the model to reproduce the measured power dependent quantum efficiency of indene-C60 bisadduct (ICBA):poly(3-hexylthiophene-2,5-diyl) (P3HT) and Phenyl–C61–Butyric Acid Methyl Ester (PCBM):P3HT solar cells under short circuit conditions reported in Ref. 28. The only fitting parameters in the fitting procedure are the traps' energy, the traps' capture rate (C_nN_t), and the carriers mobility which is taken to be equal for electrons and holes. For the effective gaps we used 1.36 eV and 1.1 eV for the ICBA:P3HT and PCBM:P3HT devices, respectively.[9,28] Figure 3(a) shows the fit for the ICBA:P3HT device. The symbols are the data points reported in Ref. 28 and the line is the model's fit. As was discussed by Tzabari *et al.*[28,30,33] the first drop, at $\sim 10^{-2}$ Sun, is due to SRH recombination and the second, just below 1 Sun, is due to bimolecular type recombination. As was stated in Ref. 28, within the current model, this bi-molecular signature arises from the band bending that slows the charge extraction through the electrodes. Figure 3(b) shows a similar fit but for the PCBM:P3HT solar cell. Having obtained the parameters for the ICBA:P3HT and PCBM:P3HT device (Tables II and III in the Appendix), we changed the contact's boundary conditions to reflect open circuit instead of short circuit. The fact that recombination at the contact interface is enhanced at open circuit is implicit in the implementation of the contacts in our model and no special

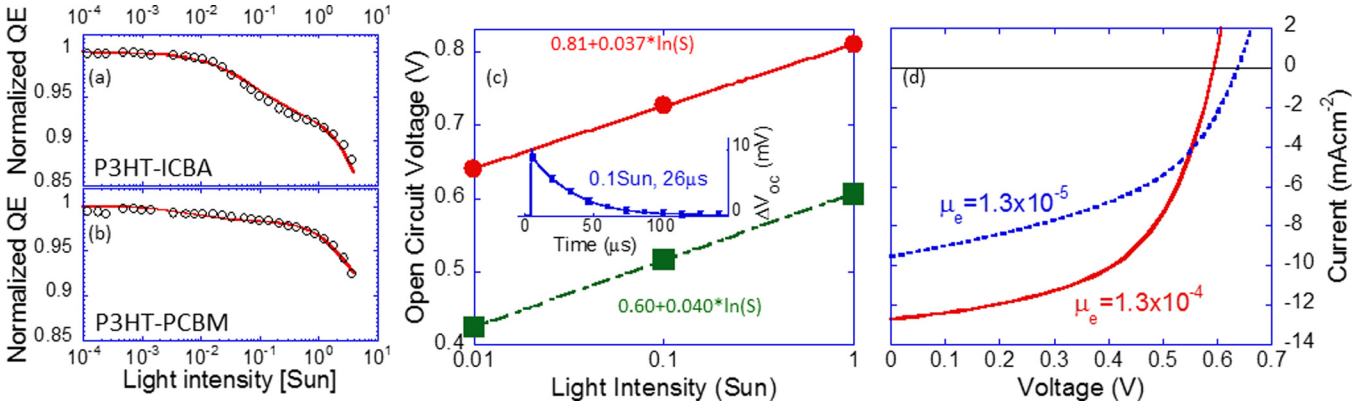

FIG. 3. (a) and (b) The simulated open circuit voltage as a function of the excitation light intensity for P3HT-ICBA (squares) and P3HT-PCBM (circles) type devices. The values for CnNt used to simulate the ICBA and PCBM devices were 9.3×10^4 and 2.8×10^4, respectively. (c) Light intensity dependent open circuit voltage for the ICBA (round symbols) and PCBM (square symbols) devices. Inset shows the transient photo voltage simulation of the ICBA device at 0.1 Sun (the time constant found here is 20 μs). (d) Simulated current voltage curves under one Sun illumination for the P3HT:PCBM solar cell. The solid lines are for $\mu_e = \mu_h = 1.3 \times 10^{-4}$ cm^2/V s and the dashed line is for the case where the electron mobility only is reduced by a factor of 10.

ad-hoc changes are required. Figure 3(c) shows the excitation density dependence of the open circuit voltage. The round symbols are data points calculated for ICBA:P3HT and the square symbols are for PCBM:P3HT. The full line is the fit to $V_{OC} = V_{OC1Sun} + n_{id}kT\ln(S)$ where V_{OC1Sun} is the open circuit at 1 Sun illumination, n_{id} is the ideality factor, kT is the thermal energy, and S is the illumination intensity in Sun units. The data for PCBM:P3HT is in good agreement with reports of the V_{OC} dependence on light intensity.[34,35] The inset to Figure 3(c) shows the simulated transient photo voltage (TPV) for the PCBM:P3HT device under 0.1 Sun. In agreement with Ref. 35 this is a mono-exponential decay.

As the last example of showing the model to be sufficient we also examine the report by Vandewal *et al.*[36] which showed that by reducing the donor concentration below its optimum value, the open circuit voltage increased at the expense of a reduced short-circuit current. The interpretation given was that the reduction of bulk recombination and the change in open circuit voltage are solely due to a reduced interface area. This may seem to contradict our claim that there are other factors affecting V_{OC} too. The data reported in Ref. 36 is not sufficient for us to construct a model that would reproduce their data; hence, we only attempt to reproduce the trend. As the dilution of the C60 molecule is most likely accompanied by a reduction of the electron mobility and since the reported reduction in the leakage current could also be attributed to that, we will examine the effect of reducing the electron mobility while keeping the bulk (SRH) recombination unchanged. The solid line in Figure 3(d) is the simulated current voltage curves under one Sun illumination for the P3HT:PCBM solar cell simulated in Figures 3(b) and 3(c) ($\mu_e = \mu_h = 1.3 \times 10^{-4}$ cm^2/V s). The dashed line is for the case where the electron mobility only is reduced by a factor of 10. We note that the effect is very similar to that reported in Ref. 36 suggesting that the mechanism suggested here could also be, at least part of, a valid explanation of the data.

New device structure

Having established the credibility of the model we reiterate that the results presented in Figure 2 imply that the charge density at the electrode interface is preventing the Fermi level from going higher towards the band edges. This limits the energy gap between the two electrodes and consequently, limits the open circuit voltage. To address this issue and suggest a solution we first write the expression for the interfacial electron density right at the electrode: $n_e(0) = N_C \exp\left(-\frac{E_C - E_{FMe}}{kT}\right)$. Here $n_e(0)$ is the density close to the electron collecting electrode and E_{FMe} is the contact work function. A similar expression can be written for the hole collecting electrode. In the context of the above expression the problem we need to solve is how to raise the contact work function (E_{FMe}) while avoiding the exponential increase in $n_e(0)$. To raise E_{FMe} without increasing the charge density one needs to compensate by either reducing the density of states, N_C, accordingly or by raising E_C such that the barrier height at the electrode (E_C-E_{FMe}) would not decrease. Conceptually, is seems that the simplest way to reduce the density of states for electrons close to the cathode is to dilute the acceptor material in a region close to the electrode by either reducing its concentration relative to that of the donor or by adding an inert (high bandgap) material. However, in practice, it is difficult to precisely control the dilution ratio and moreover, chemical processes that pin the electrode and are not part of the analysis above would still be active as the electron conducting material is unchanged. Indeed such methods have been tried before and resulted in only a minor enhancement of the open circuit voltage. The study by Guerrero *et al.*[26] has indeed shown that the addition of $PC_{60}BM$ or $PC_{70}BM$ to P3HT affects the flat-band voltage and that it reduces with the increase in concentration of the PCBM molecule.

Alternatively, one could use for the region close to the electrode an acceptor material with a higher LUMO (E_C) level. This method is more easily realizable and is capable of rectifying the effect of other electrode-pinning mechanisms that may take place right at the interface (as the LUMO at the interface is raised). However, the most important advantage of this method is that the energy difference between the LUMO level at the cathode interface and the HOMO level at the anode interface is increased. This in turn allows to open the gap

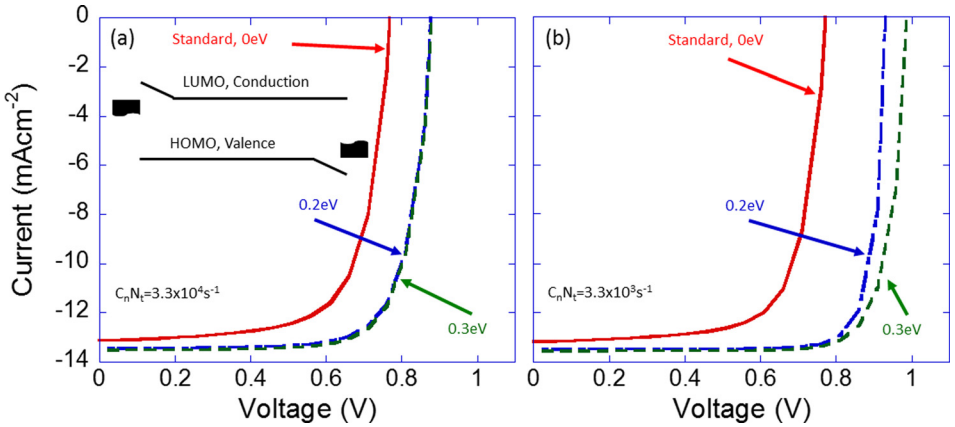

FIG. 4. The inset to (a) shows the schematic band diagram where the material composition at the 30 nm on each side is chosen such that the effective gap increases towards the electrode. (a) Simulated current voltage curves under one Sun illumination using the SRH recombination rate typical for P3HT based BHJ devices ($C_nN_t = 3.3 \times 10^4\ s^{-1}$) and using the device parameters of the ICBA:P3HT device. The I-V curves are for the standard flat band device (red, full line), the device with a 0.2 eV increase of the bandgap at the electrodes (blue, dashed-dotted), and for a 0.3 eV increase (green, dashed). (b) The same as in (a) but assuming an improved material system where the recombination rate is reduced by a factor of 10 relative to P3HT based material systems. The improvement in PCE predicted in (a) and (b) are 28% and 45%, respectively.

between the two electrodes' energy and thus enhance the built-in potential almost independently of the HOMO-LUMO gap in the bulk of the device (see inset to Figure 4(a)).

The inset to Figure 4(a) schematically illustrates the concept of shifting the relevant energy level in the vicinity of the respective contact. The illustration suggests that towards the electron collecting electrode the acceptor material is changed to one with a higher LUMO level and that towards the hole collecting electrode the donor material is replaced by one with a deeper HOMO level. As the inset shows, this structure implements what seems to be a barrier for charge extraction which is known to be detrimental for the cell performance.[37] However, since we take advantage of the energy level shift to also shift the electrode work function (contact barrier at the interface is unchanged) this work function shift, and the resulting higher built-in potential, more than compensates for the alleged barrier (see Figures 5 and 6 in the Appendix). At first glance, the structure drawn at the inset of Figure 4(a) seems similar to the one reported in Ref. 5. However, since the motivation in Ref. 5 was exciton management the energy level gradient at the anode interface was induced in the LUMO level while for our purpose the gradient has to be induced at the HOMO level.

To demonstrate the effect we implemented in our simulations a gradual linear shift in the levels as is shown in the inset to Figure 4(a) and extended it over 30 nm close to the electrode only. In practice this could be a stepwise increase using several available material derivatives as shown in Tables IV and V in the Appendix. Figure 4(a) shows the simulated current voltage curves under one Sun illumination using the SRH recombination rate typical for P3HT based BHJ devices ($C_nN_t = 3.3 \times 10^4\ s^{-1}$) and using the device parameters of the ICBA:P3HT device. The I–V curves are for the standrad flat band device (red, full line), the device with 02 eV increase of the bandgap at the electrodes (blue, dashed-dotted), and for 0.3 eV increase (green, dashed). As the barrier height at the interface is unchanged and is kept at 0.2 eV, the energy gap between the two contacts is shifting from 0.96 eV to 1.36 eV and to 1.56 eV. We note that for P3HT based systems one can expect a 28% enhancement in power conversion efficiency (PCE) which is due to a 0.1 V increase in V_{OC} as well as an improved fill factor.

In Figure 4(b) we test the potential of this method for material systems exhibiting better performance with respect to P3HT based ones. We make only the reasonable assumption that such an improved system would possess a 10 fold lower recombination rate and keep all other parameters identical. The overall increase in PCE shown in Figure 4(b) is now predicted to be 48% which is due to a 0.2 V (~26%) increase in V_{OC} and an improved fill factor (by 17%).

SUMMARY AND CONCLUSIONS

To conclude, it was the aim of this contribution to deliver the message that the advanced materials developed for BHJ devices have a huge potential yet to be uncovered and that the performance of high efficiency devices (at least those of 10% or above) is most likely limited by the device structure and not by the materials' properties. One such device property is the pinning of the electrode work function below the energy level of the bulk of the device which effectively limits the built-in potential of the device. By modifying the material composition at the vicinity of the electrode we open the possibility to enhance the energy gap between the electrodes and thus also the built-in potential.

The calculations presented in the Appendix (Figure 6) and in Figure 4(a) indicate that the PCE of P3HT based systems could be improved by up to 28%. The calculations shown in Figure 4(b) indicate that higher quality material compositions[4] may show up to a 0.20 V increase in their open circuit voltage which together with the improved fill factor would lead to a 48% increase in their power conversion efficiency. We find the prospect of going from 10% to 15% efficiency through device structuring most promising.

ACKNOWLEDGMENTS

We acknowledge the support of the Israeli Nanotechnology Focal Technology Area on Nanophotonics for Detection, the Grand Technion Energy Program (GTEP), and comprises part of The Leona M. and Harry B. Helmsley Charitable Trust reports on Alternative Energy series of the Technion, Israel Institute of Technology, and the Weizmann Institute of Science.

APPENDIX: SIMULATION DETAILS AND PARAMETERS

The full set of parameters used in the simulations are collected into the tables below.

To better understand the new device structure suggested in the paper we introduce it in two steps. First, we examine the case where only the semiconductor close to the contacts is modified and next we show an improved structure where the modification of the semiconductor close to the contacts is

TABLE I. Parameters used to simulate the reference devices (full line, red) in Figure 2.

Parameter	Value
Eg effective (eV)	1.36
μ_e ($cm^2\ V^{-1}\ s^{-1}$)	10^{-3}
μ_h ($cm^2\ V^{-1}\ s^{-1}$)	10^{-3}
$C_n * N_t$ (s^{-1})	3.3×10^5
$2n_i \cosh\left(\frac{\Delta E_t}{kT}\right)$	$10^{15}\,cm^{-3}$
E_C-E_{FMe} (eV)	−0.2
E_V-E_{FMh} (eV)	0.2

TABLE II. Parameters used to simulate the P3HT:ICBA device in Figure 3 of the paper. The values that were obtained through fitting the intensity dependent efficiency are marked.

Parameter	Value
Eg effective (eV)	1.36
μ_e ($cm^2\ V^{-1}\ s^{-1}$)	1.5×10^{-4} (fitted parameter)
μ_h ($cm^2\ V^{-1}\ s^{-1}$)	1.5×10^{-4} (fitted parameter)
$C_n * N_t$ (s^{-1})	9.3×10^4 (fitted parameter)
$2n_i \cosh\left(\frac{\Delta E_t}{kT}\right)$	$10^{15}\,cm^{-3}$ (fitted parameter)
E_C-E_{FMe} (eV)	−0.2
E_V-E_{FMh} (eV)	0.2

TABLE III. Parameters used to simulate the P3HT:PCBM device in Figure 3 of the paper. The values that were obtained through fitting the intensity dependent efficiency are marked.

Parameter	Value
Eg effective (eV)	1.1
μ_e ($cm^2\ V^{-1}\ s^{-1}$)	1.3×10^{-4} (fitted parameter)
μ_h ($cm^2\ V^{-1}\ s^{-1}$)	1.3×10^{-4} (fitted parameter)
$C_n * N_t$ (s^{-1})	2.8×10^4 (fitted parameter)
$2n_i \cosh\left(\frac{\Delta E_t}{kT}\right)$	$1.46 \times 10^{14}\,cm^{-3}$ (fitted parameter)
E_C-E_{FMe} (eV)	0.0
E_V-E_{FMh} (eV)	0.2

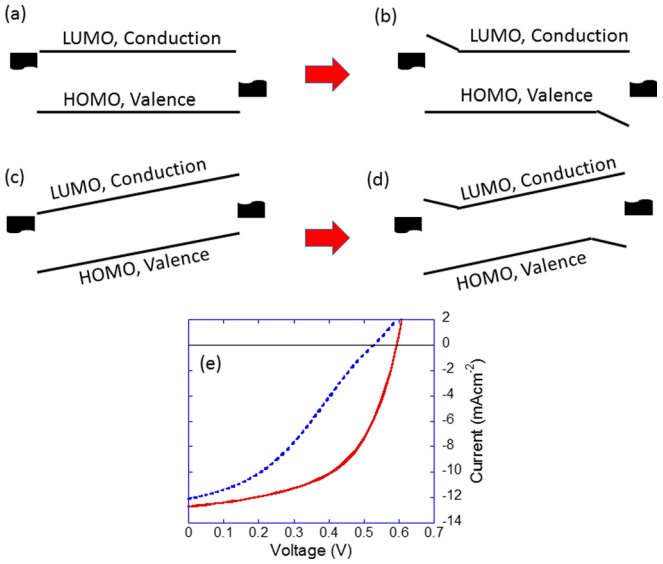

FIG. 5. (a)–(d) Schematic description of the energy band diagram of the simulated devices. The standard uniform bulk-heterojunction device at open circuit (a) and at short circuit (c). Open circuit (b) and short circuit (d) band diagrams of the modified device structure. Here, close to the cathode (anode) the acceptor (donor) is replaced by a material with a higher (lower) LUMO (HOMO) level. Note that as the contacts were not changed the band bending under short circuit conditions is unchanged too. (e) Simulated current voltage curves under one Sun illumination using the material parameters of the P3HT:PCBM device (Table III). The full line (red) is for the standard device structure and the dashed line (blue) is for the modified sructure.

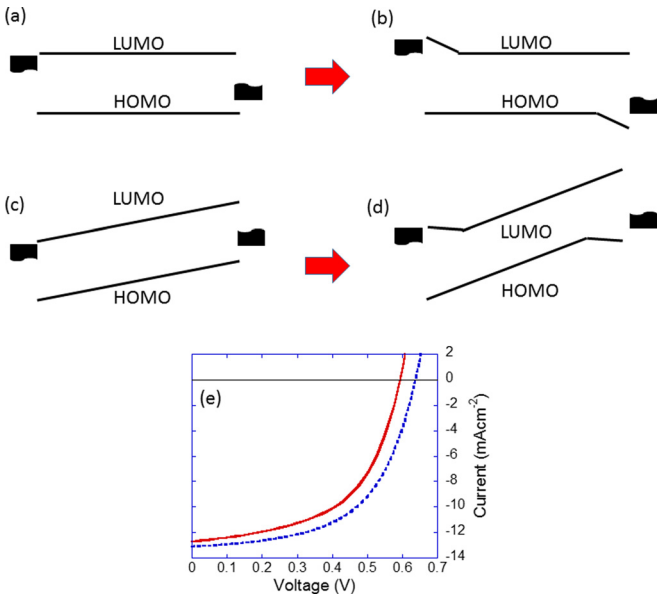

FIG. 6. (a)–(d) Schematic description of the energy band diagram of the simulated devices. (a) The standard uniform bulk-heterojunction device at open circuit and (c) at short circuit. (b) Open circuit and (d) short circuit band diagrams of the improved device structure. Here, close to the cathode (anode) the acceptor (donor) is replaced by a material with a higher (lower) LUMO (HOMO) level. The electrode work function is changed to maintain the same barrier at the contacts. (e) Simulated current voltage curves under one Sun illumination using the material parameters of the P3HT-PCBM device (Table III). The full line (red) is for the standard device structure and the dashed line (blue) is for the improved sructure.

TABLE IV. Hole transport materials that could be used to create the required slope in the HOMO level close to the anode.[37]

Material's short name	HOMO level (eV)
Spiro-MeO-TAD	5.0
Spiro-MeO-TPD	5.1
Spiro-TTB	5.3
Spiro-TAD	5.5

TABLE V. Electron transport materials that could be used to create the required slope in the LUMO level close to the cathode.

Material's short name	LUMO level relative to PCBM (eV)
PCBM	0
bisPCBM	−0.1[38]
ICBA	−0.2[39]
C60(OCH3)4-PCBM	−0.3[40]

utilized to enhance the energy gap between the electrodes (E_{FMe}-E_{FMh}). The results in Fig. 5(e) compare the simulated PCE curves of the standard P3HT:PCBM device (full line, red) with that of the modified structure where the material close to the electrodes is changed such that the gap towards the electrode was increased by 0.3 eV (dashed line, blue). For the material parameters we use those extracted in the main paper and summarized in Table III. The energy band diagram of the two device structures under open and short circuit conditions are shown in Figures 5(a)–5(d). Note that as the contacts are the same between the two structures (same work functions) the band bending at short-circuit is identical. As would be expected, from the modified structure, the enhanced barrier at the contacts reduces the short circuit current and the increase in the gap towards the electrodes impedes the charge extraction giving rise to a slight S shape. As a result, the power conversion efficiency is severely reduced.

Figure 6(e) shows the results when the improved structure is such that we take advantage of the larger gap close to the electrodes to use a cathode (anode) with a higher (lower) work function. In the improved structure the shift close to the electrode is of 0.3 eV and the electrodes are also shifted in the same manner to maintain the same barrier at the contact interface. The structural differences are shown in Figures 6(a)–6(d). In Figures 6(a) and 6(b) we compare the flat band conditions (open circuit) which illustrate how we utilize the improved structure to increase the energy gap between the electrodes (E_{FMe}-E_{FMh}). In Figures 6(c) and 6(d) we compare the equilibrium dark conditions (short circuit) which shows how the enhanced electrode gap results in a steeper band bending. As Figure 6(e) shows, both the open-circuit voltage (V_{OC}) and the short-circuit current (I_{SC}) are enhanced. The calculated enhancement of the cell's power conversion efficiency is slightly above 14%.

[1]K. M. Coakley and M. D. McGehee, Chem. Mater. **16**, 4533 (2004).
[2]U. Wurfel, D. Neher, A. Spies, and S. Albrecht, Nat. Commun. **6**, 6951 (2015).
[3]N. C. Giebink, G. P. Wiederrecht, M. R. Wasielewski, and S. R. Forrest, Phys. Rev. B **83**, 195326 (2011).
[4]Y. Liu, J. Zhao, Z. Li, C. Mu, W. Ma, H. Hu, K. Jiang, H. Lin, H. Ade, and H. Yan, Nat. Commun. **5**, 5293 (2014).
[5]O. L. Griffith and S. R. Forrest, Nano Lett. **14**, 2353 (2014).
[6]D. Veldman, S. C. J. Meskers, and R. A. J. Janssen, Adv. Funct. Mater. **19**, 1939 (2009).
[7]M. C. Scharber, D. Mühlbacher, M. Koppe, P. Denk, C. Waldauf, A. J. Heeger, and C. J. Brabec, Adv. Mater. **18**, 789 (2006).
[8]J. Widmer, M. Tietze, K. Leo, and M. Riede, Adv. Funct. Mater. **23**, 5814 (2013).
[9]R. A. Street, S. A. Hawks, P. P. Khlyabich, G. Li, B. J. Schwartz, B. C. Thompson, and Y. Yang, J. Phys. Chem. C **118**, 21873 (2014).
[10]M. C. Scharber and N. S. Sariciftci, Prog. Polym. Sci. **38**, 1929 (2013).
[11]S. D. Dimitrov and J. R. Durrant, Chem. Mater. **26**, 616 (2014).
[12]F. Ortmann, K. S. Radke, A. Gunther, D. Kasemann, K. Leo, and G. Cuniberti, Adv. Funct. Mater. **25**, 1933 (2015).
[13]C. Poelking, K. Daoulas, A. Troisi, and D. Andrienko, in *P3HT Revisited: From Molecular Scale to Solar Cell Devices*, edited by S. Ludwigs (Springer-Verlag, Berlin, 2014), Vol. 265, p. 139.
[14]G. Lakhwani, A. Rao, and R. H. Friend, Annu. Rev. Phys. Chem. **65**, 557 (2014).
[15]Y. Olivier, D. Niedzialek, V. Lemaur, W. Pisula, K. Mullen, U. Koldemir, J. R. Reynolds, R. Lazzaroni, J. Cornil, and D. Beljonne, Adv. Mater. **26**, 2119 (2014).
[16]L. Dou, J. You, Z. Hong, Z. Xu, G. Li, R. A. Street, and Y. Yang, Adv. Mater. **25**, 6642 (2013).
[17]B. Kippelen and J. L. Bredas, Energy Environ. Sci. **2**, 251 (2009).
[18]W. Shockley and H. J. Queisser, J. Appl. Phys. **32**, 510 (1961).
[19]J. Xue, S. Uchida, B. P. Rand, and S. R. Forrest, Appl. Phys. Lett. **84**, 3013 (2004).
[20]W. J. Potscavage, S. Yoo, and B. Kippelen, Appl. Phys. Lett. **93**, 193308 (2008).
[21]J. Bisquert, Phys. Chem. Chem. Phys. **10**, 3175 (2008).
[22]T. Kirchartz and U. Rau, Phys. Status Solidi A **205**, 2737 (2008).
[23]K. Vandewal, Z. F. Ma, J. Bergqvist, Z. Tang, E. G. Wang, P. Henriksson, K. Tvingstedt, M. R. Andersson, F. L. Zhang, and O. Inganas, Adv. Funct. Mater. **22**, 3480 (2012).
[24]U. Rau, Phys. Rev. B **76**, 085303 (2007).
[25]J. Hwang, A. Wan, and A. Kahn, Mater. Sci. Eng., R **64**, 1 (2009).
[26]A. Guerrero, L. F. Marchesi, P. P. Boix, S. Ruiz-Raga, T. Ripolles-Sanchis, G. Garcia-Belmonte, and J. Bisquert, ACS Nano **6**, 3453 (2012).
[27]N. Tessler, J. Polym. Sci., Part B: Polym. Phys. **52**, 1119 (2014).
[28]L. Tzabari, J. Wang, Y.-J. Lee, J. W. P. Hsu, and N. Tessler, J. Phys. Chem. C **118**, 27681 (2014).
[29]D. Wing, A. Rothschild, and N. Tessler, J Appl. Phys. **118**, 054501 (2015).
[30]L. Tzabari, V. Zayats, and N. Tessler, J. Appl. Phys. **114**, 154514 (2013).
[31]R. A. Street, A. Krakaris, and S. R. Cowan, Adv. Funct. Mater. **22**, 4608 (2012).
[32]S. R. Cowan, W. L. Leong, N. Banerji, G. Dennler, and A. J. Heeger, Adv. Funct. Mater. **21**, 3083 (2011).
[33]L. Tzabari and N. Tessler, J. Appl. Phys. **109**, 064501 (2011).
[34]S. A. Hawks, G. Li, Y. Yang, and R. A. Street, J. Appl. Phys. **116**, 074503 (2014).
[35]C. G. Shuttle, B. O'Regan, A. M. Ballantyne, J. Nelson, D. D. C. Bradley, J. de Mello, and J. R. Durrant, Appl. Phys. Lett. **92**, 093311 (2008).
[36]K. Vandewal, J. Widmer, T. Heumueller, C. J. Brabec, M. D. McGehee, K. Leo, M. Riede, and A. Salleo, Adv. Mater. **26**, 3839 (2014).
[37]L. E. Polander, P. Pahner, M. Schwarze, M. Saalfrank, C. Koerner, and K. Leo, APL Mater. **2**, 081503 (2014).
[38]G.-J. A. H. W. F. B. K. S. C. V. J. C. H. P. W. M. B. Martijn Lenes, Adv. Mater. **20**, 2116 (2008).
[39]Y. He, H.-Y. Chen, J. Hou, and Y. Li, J. Am. Chem. Soc. **132**, 1377 (2010).
[40]L.-L. Deng, S.-L. Xie, C. Yuan, R.-F. Liu, J. Feng, L.-C. Sun, X. Lu, S.-Y. Xie, R.-B. Huang, and L.-S. Zheng, Sol. Energy Mater. Sol. Cells **111**, 193 (2013).